Chapter 8

Aberrations

In the analysis presented previously, the mathematical models were developed assuming perfect lenses, i.e. the lenses were clear and free of any defects which modify the propagating optical wavefront. However, it is interesting to investigate the effects that departures from such ideal cases have upon the resolution and image quality of a scanning imaging system. These departures are commonly referred to as aberrations [23]. The effects of aberrations in optical imaging systems is a immense subject and has generated interest in many scientific fields, the majority of which is beyond the scope of this thesis. Hence, only the common forms of aberrations evident in optical storage systems will be discussed.

Two classes of aberrations are defined, monochromatic aberrations - where the illumination is of a single wavelength, and chromatic aberrations - where the illumination consists of many different wavelengths. In the current analysis only an understanding of monochromatic aberrations and their effects is required [4], since a source of illumination of a single wavelength is generally employed in optical storage systems.

The following chapter illustrates how aberrations can be modelled as a modification of the aperture pupil function of a lens. The mathematical and computational procedure presented in the previous chapters may then be used to determine the effects that aberrations have upon the readout signal in optical storage systems. Since the analysis is primarily concerned with the understanding of aberrations and their effects in optical storage systems, only the response of the Type 1 reflectance and Type 1 differential detector MO scanning microscopes will be investigated.

8.1 The origins of aberrations

The mathematical foundation of aberrations is described using ray and geometrical optics, which is presented in many texts [23,43,106,107]. However, a simple description of the origins of aberrations will be presented which will aid in the understanding of aberrations and how their effects can be modelled as an introduction of a phase factor into the function representing the aperture pupil function of the perfect lens.

If rays from a point source are traced through an optical system such that each ray travels the same distance as the chief ray (that ray which travels along the optical axis), then the surface that can be traced through the ray end points is termed the optical wavefront. The optical wavefront is ideally spherical in shape, the radius of which is determined by the optical path length of the chief ray. If the wavefront deviates from this ideal spherical case then the wavefront is said to be aberrated. Figure 8.1 illustrates the ideal spherical wavefront and the aberrated wavefront.
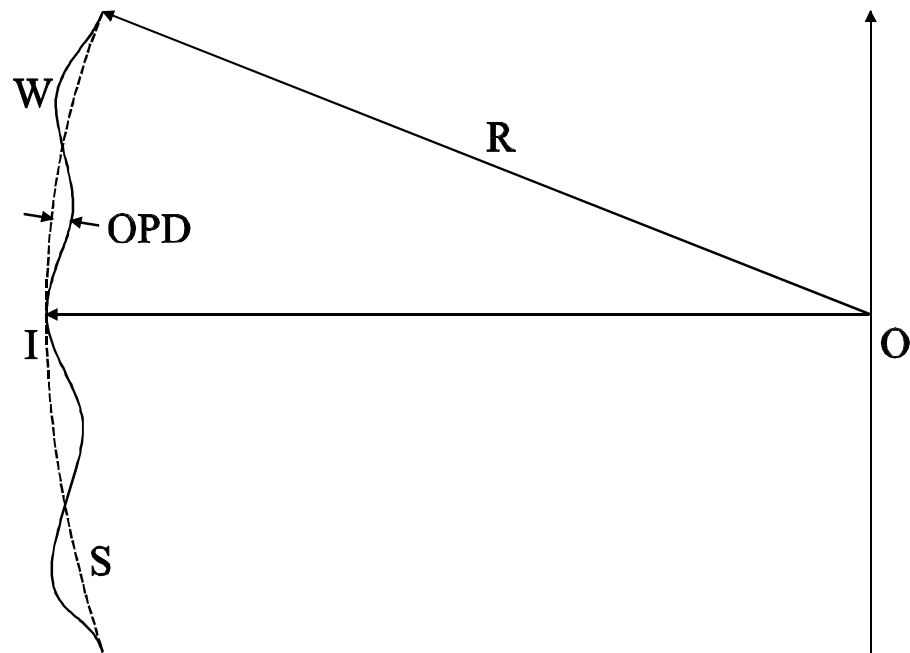

Figure 8.1 : *The ideal spherical wavefront (dashed line) and the aberrated wavefront (solid).*

The aberrated wavefront, *W*, at the image point, *I*, for an object placed at the origin, *O*, is illustrated as the deviation from the ideal spherical wavefront, *S*. The optical

path difference, *OPD*, is the distance along a ray between the spherical wavefront and the aberrated wavefront. If the wavefront is travelling through a medium of refractive index, *n*, then the aberration is given by *n* multiplied by the optical path difference.

Aberrations in lenses are due to imperfections inherently introduced during the manufacturing process, the majority of which are eliminated by careful design [60]. However, aberrations may be introduced due to other sources in the optical system, such as birefringence and spherical aberration in disc substrates and defocus in optical disc systems.

Aberrations in a thin lens are modelled as an introduction of a phase factor into the aperture pupil function of the perfect lens. Due to the radial symmetry of a circular lens it is common to express the aperture pupil function in polar co-ordinates, i.e. (r, f). The aperture pupil function of the aberrated lens is given by

$$p'(r, f) = p(r, f) \exp\{2pj W(r, f)\} \tag{8.1}$$

where $p(r, f)$ is the aperture pupil function of the ideal, aberration free, lens, $p'(r, f)$ is the modified aperture pupil function due to the introduction of aberrations and $W(r, f)$ is the aberration function. The complex aberration function describes the variations of the wavefront across the surface of the lens and is expressed in units of wavelength, λ [32,60,107]. The aberration function may be expressed as an expansion of a binomial series, referred to as Zernike's polynomials, the terms of which correspond to different forms of aberration [60,107]. The primary aberrations, or Seidel aberrations as they often called, are combinations of the Zernike polynomials that describe the common forms of aberrations, i.e. defocus, spherical aberration, astigmatism, coma and tilt. The aberration function may be expressed as a function of these primary aberrations, i.e.

$$W(r, f) = A_S r^4 + A_A r^3 \cos(f) + A_C r^2 \cos^2(f) + A_D r^2 + A_T r \cos(f) \tag{8.2}$$

where r is the normalised distance from the centre of the aperture, $r = r / a$ where a is the radius of the circular aperture, and A_i are the aberration coefficients. The range of values for r and f are given by $0 \le r \le 1$ and $0 \le f < 2p$, the peak aberration

coefficient occurring at the edge of the aperture pupil. The aberration coefficients each represent one of the primary aberrations, i.e.

$$A_S \quad : \quad \text{spherical aberration}$$
$$A_A \quad : \quad \text{astigmatism}$$
$$A_C \quad : \quad \text{coma}$$
$$A_D \quad : \quad \text{defocus}$$
$$A_T \quad : \quad \text{tilt}$$

where the aberration coefficients are expressed in units of wavelength, λ.

Substituting eq. (8.2) into eq. (8.1) allows the modified aperture pupil function to be expressed as a function of the primary aberrations. Hence, the effects of each form of aberration can be investigated by substituting a value for the appropriate aberration coefficient in the aberrated aperture pupil function.

8.2 Aberrations in optical storage systems

In the following section, the effects due to sources of aberrations in optical storage systems will be described, namely: defocus, spherical aberrations and astigmatism.

8.2.1 Defocus

In optical storage systems the incident field of illumination is brought to focus, through the substrate of the disc, onto the information layer by the objective lens. As the disc rotates the plane of the information layer oscillates due to imperfections in the disc or simply because the disc is not flat. If the information layer remains within the focal point of the lens then these variations will have little, if any, effect. However, if the movement is large, such that information layer moves away from the focal point of the lens, then the signal from the system will be degraded due to defocus [18,32,60]. In optical disc systems, the effects of defocus are ameliorated by using automatic focusing techniques to ensure that the information layer remains within the focal point of the lens. This is achieved by mounting the objective lens in an actuator system, the

position of which is controlled by a closed loop feedback control system. However, as new generations of optical disc systems are developed, such as DVD, where greater storage capability is achieved by reducing the wavelength of illumination and increasing the NA of the objective lens, the effects of defocus upon the readout signal becomes more severe, since the depth of focus, l / NA^2, decreases correspondingly. Knowledge of the effects on the readout signal due to defocus is therefore important and is described in the following section.

It has been discussed in chapter 2 that the far-field diffraction pattern can be used to represent the field distribution at the focal point of a thin lens. However, the expression given by eq. (2.32) is obtained by simply replacing the distance co-ordinate, z in eq. (2.31), with the focal length of the lens, f, assuming the lens is in perfect focus. However, what would be the effect if the point of observation is not at the focal point of the lens, such as when the lens is defocused? In this case the simplification of eq. (2.31) will not hold and the field distribution at the observation point can not be represented by eq. (2.32).

The modified field distribution due to defocus can be calculated by returning to eq. (2.31) and expanding the terms in the integral to give

$$
\begin{aligned}
\mathbf{y}(x_2, y_2) = {} & \frac{\exp\{-jkz\}}{jlz} \exp\left\{\frac{-jk}{2z}(x_2^2 + y_2^2)\right\} \\
& \cdot \iint\limits_{-\infty}^{\infty} p_1(x_1, y_1) \exp\left\{\frac{-jk}{2z}(x_1^2 + y_1^2)\right\} \exp\left\{\frac{jk}{2f}(x_1^2 + y_1^2)\right\} \\
& \cdot \exp\left\{\frac{jk}{z}(x_2 x_1 + y_2 y_1)\right\} dx_1 dy_1
\end{aligned}
\tag{8.3}
$$

which by further modification gives

$$
\begin{aligned}
\mathbf{y}(x_2, y_2) = {} & \frac{\exp\{-jkz\}}{jlz} \exp\left\{\frac{-jk}{2z}(x_2^2 + y_2^2)\right\} \iint\limits_{-\infty}^{\infty} p_1(x_1, y_1) \\
& \cdot \exp\left\{\frac{jk}{2}(x_1^2 + y_1^2)\left[\frac{1}{f} - \frac{1}{z}\right]\right\} \exp\left\{\frac{jk}{z}(x_2 x_1 + y_2 y_1)\right\} dx_1 dy_1
\end{aligned}
\tag{8.4}
$$

where the far-field diffraction pattern, $\mathbf{y}(x_2, y_2)$, is that observed in the plane $\{x_2, y_2\}$ a distance z from the plane of the lens, $\{x_1, y_1\}$, where $z \neq f$.

If the point of observation of the far field diffraction pattern is a distance df from the focal point of the lens, i.e. $z=f+df$ where $f >> df$, then substituting for z into eq. (8.4) gives

$$
\mathbf{y}(x_2, y_2) = \frac{\exp\{-jk(f + df)\}}{jl(f + df)} \exp\left\{\frac{-jk}{2(f + df)}(x_2^2 + y_2^2)\right\}
$$

$$
\cdot \iint\limits_{-\infty}^{\infty} p_1(x_1, y_1) \exp\left\{\frac{jk}{2z}(x_1^2 + y_1^2)\left[\frac{1}{f} - \frac{1}{(f + df)}\right]\right\}
$$

$$
\cdot \exp\left\{\frac{jk}{(f + df)}(x_2 x_1 + y_2 y_1)\right\} dx_1 dy_1
$$

(8.5)

However, by substituting for

$$
\left[\frac{1}{f} - \frac{1}{(f + df)}\right] \equiv \frac{df}{f(f + df)}
$$

(8.6)

into eq. (8.5) and re-arranging

$$
\mathbf{y}(x_2, y_2) = \frac{\exp\{-jkf\}}{jlf} \exp\left\{\frac{-jk}{2f}(x_2^2 + y_2^2)\right\}
$$

$$
\cdot \iint\limits_{-\infty}^{\infty} p_1(x_1, y_1) \exp\left\{\frac{jk\,df}{2f^2}(x_1^2 + y_1^2)\right\} \exp\left\{\frac{jk}{f}(x_2 x_1 + y_2 y_1)\right\} dx_1 dy_1
$$

(8.7)

assuming $f >> df$.

Hence, comparing eq. (8.7) and eq. (2.32) it can be seen that the expression representing the field distribution in the plane a distance df from the focal point of a lens is similar to that expression representing the field distribution in the ideal focal point of a lens. However, the extra exponential term in the integral of eq. (8.7) describes the wavefront aberration in the lens due to the defocus, df. Comparing eq. (8.7) and eq. (2.32) it can be seen that the aperture pupil function of the defocused lens is given by

$$
p'(x_1, y_1) = p(x_1, y_1) \exp\left\{\frac{jk\,df}{2f^2}(x_1^2 + y_1^2)\right\}
$$

(8.8)

and the aberration coefficient, A_D, due to the defocus, df, is given by

$$
A_D = \frac{df\,a^2}{2f^2} \approx \frac{NA^2 df}{2}
$$

(8.9)

where *NA* is the numerical aperture of the lens. Substituting eq. (8.9) into eq. (8.7) gives

$$
\mathbf{y}(x_2, y_2) = \frac{\exp\{-jkf\}}{j\mathbf{l}f} \exp\left\{\frac{-jk}{2f}\left(x_2^2 + y_2^2\right)\right\}
$$

$$
\cdot \iint\limits_{-\infty}^{\infty} p_1(x_1, y_1) \exp\left\{\frac{j2\mathbf{p}A_D}{\mathbf{l}}\frac{\left(x_1^2 + y_1^2\right)}{a^2}\right\} \exp\left\{\frac{jk}{f}\left(x_2 x_1 + y_2 y_1\right)\right\} dx_1 dy_1
$$

$$(8.10)$$

which is the modified amplitude point spread function due to a lens which is defocused by an amount $\mathbf{d}f$.

Using eq. (8.10) it is possible to calculate the resulting point spread function due to a lens defocused by an amount $\mathbf{d}f$. The aberration function, A_D, is calculated for a known amount of defocus, $\mathbf{d}f$, using eq. (8.9), where A_D is in units of wavelength. For example, for a defocus of $\mathbf{d}f = 2.56\mathbf{m}m$, an NA of 0.5 and a wavelength $0.8\mathbf{m}m$, the defocus aberration coefficient is given by $0.4\mathbf{l}$. This results in the focused spot profile illustrated in Fig. 8.2.
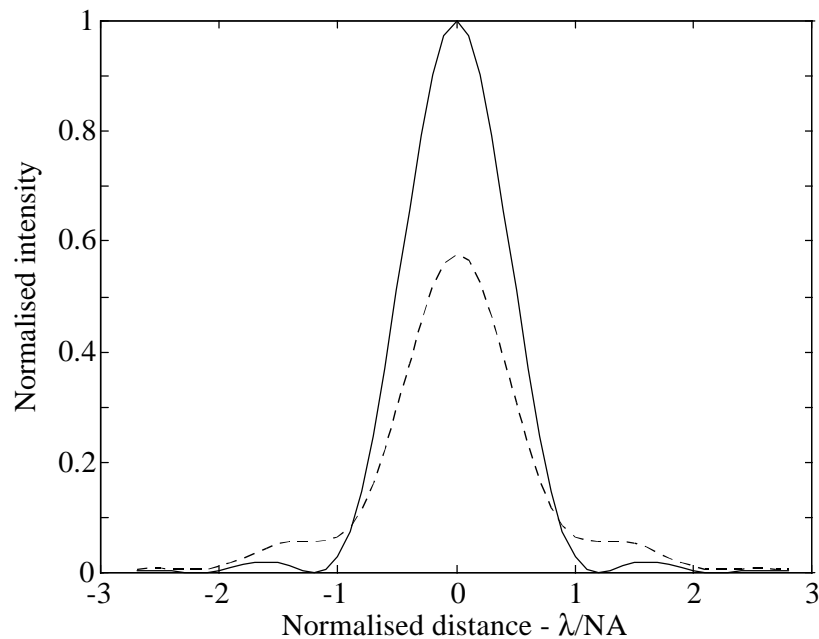

Figure 8.2 : *The point spread function for a clear circular lens under uniform illumination for 0.4**l** defocus (dashed line). Also illustrated is a plot of the ideal point spread function (solid line).*

Figure 8.2 illustrates that a small amount of defocus can have a large effect upon the resolution and intensity of the focused spot. In this example the intensity of the focused spot has been reduced by nearly 50%, and the width of the spot has been increased by the added intensity contribution due to the sidelobes of the defocused spot.

The defocused point spread function

The resolution of the scanning optical system is determined primarily by the width and profile of the point spread function. It has been shown previously that the point spread function, and hence, the focused spot, is a function of the aperture pupil function of the lens, the wavelength and form of the incident illumination, and the numerical aperture of the lens. However, in the defocused optical system the form of the aperture pupil function is modified by the introduction of an aberration function due to the defocus. This defocus affects the shape of the irradiance profile and hence, the resolution of the imaging system. In Fig. 8.3 contour plots of the irradiance profile of a lens are illustrated for varying degrees of defocus, for a clear, circular aperture under uniform illumination. The scale of the plots is in normalised units of l / NA. In Fig. 8.4 the axial profiles of the defocused irradiance are illustrated normalised with respect to the irradiance of the ideal case (no defocus). For a wavelength of 0.8μm and a NA 0.5 (typical optical storage values) the plots in Fig. 8.3 and Fig. 8.4 correspond to a defocus of $df = 0$ in a) to $df = 6.4$μm in f) at 1.28μm steps.

Figures 8.3 and 8.4 demonstrate that as the defocus aberration coefficient is increased the effective width of the irradiance profile increases, and becomes more diffuse, introducing rings of varying intensity. An interesting result is illustrated in Fig. 8.3 (f) where the central portion of the spot has been extinguished leaving an outer bright ring [18]. It can be deduced that a defocused optical system will offer a reduced resolution over the ideal system, such that as defocus increases small objects will no longer be resolved.
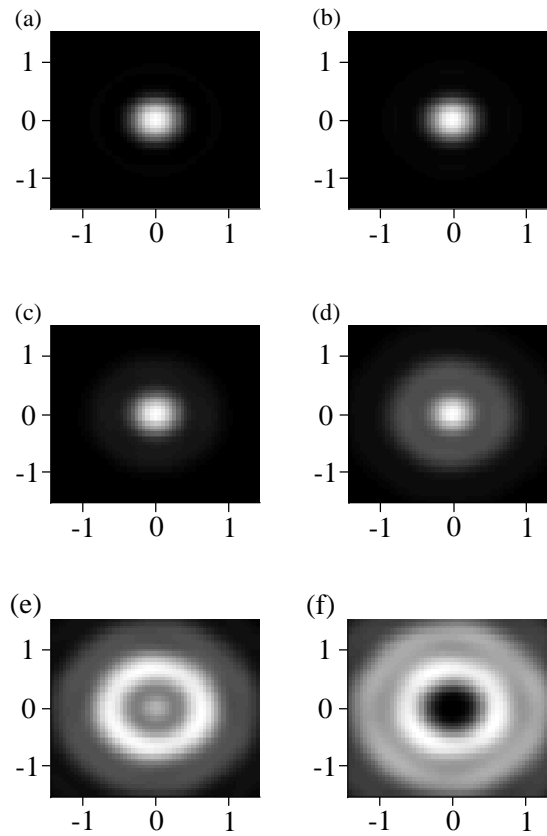
Figure 8.3 : *The irradiance profile for varying degrees of defocus. Coefficients of defocus, A_D, are a) 0, b) 0.2**l**, c) 0.4**l**, d) 0.6**l**, e) 0.8**l**, f) **1**.*
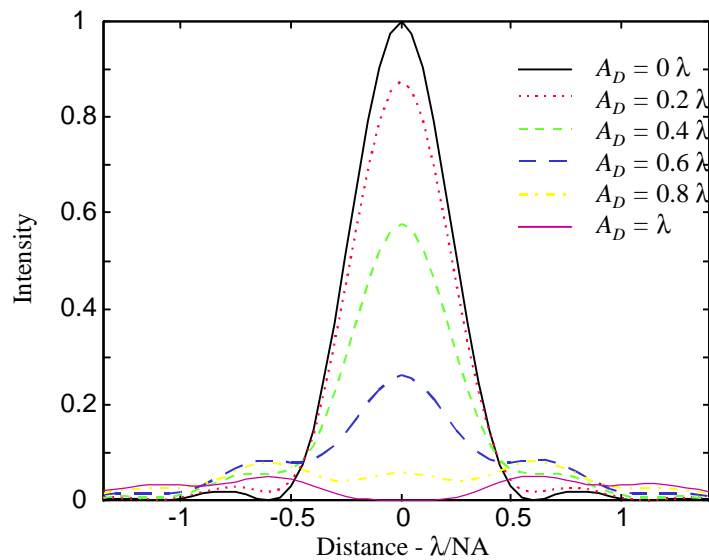

Figure 8.4 : *The irradiance profile for varying degrees of defocus.*

The defocused Type 1 PCTF

Figure 8.5 illustrates the axial form of the Type 1 PCTF, for varying degrees of defocus. The PCTFs were generated using the Type 1 PCTF algorithm with the conditions outlined in table 8.1. It should be noted that the defocus aberration is included in both the objective and collector aperture pupil functions, since in optical storage systems they are one in the same.

Objective aperture	circular - radius a
Collector aperture	circular - radius a
Incident illumination	uniform

Table 8.1
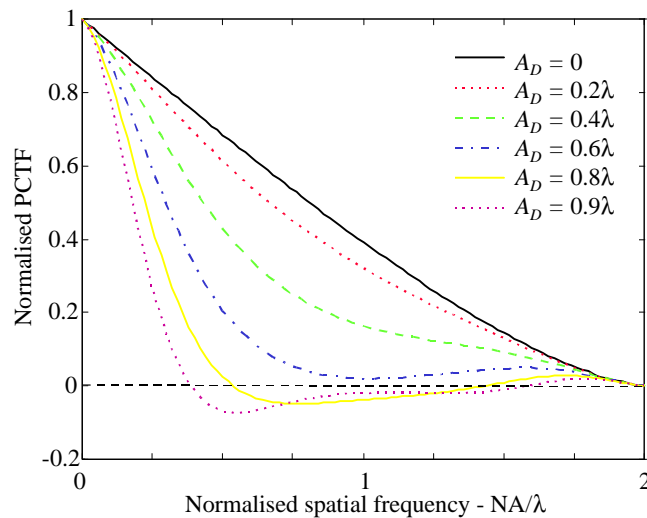
Figure 8.5 : *Normalised PCTFs for varying degrees of defocus.*

It can be seen that as the amount of defocus increases the high spatial frequency response of the Type 1 system degrades, which is to be expected due to the broadening of the amplitude point spread function. For a defocus coefficient $A_D < 0.6\lambda$ the PCTF is positive for all spatial frequencies. However, as the aberration coefficient is increased the spatial frequency response of the PCTF becomes negative. If the spatial frequency response of the PCTF is negative, then this corresponds to a phase shift of π, which is termed *contrast reversal*, since bright regions in the object to appear dark in the image, or vice versa. The result illustrated in Fig. 8.5 corresponds exactly with the results of other researchers [106,107,119,128].

The step response of the defocused optical system

Figure 8.6 and Fig. 8.7 illustrate the step response of the Type 1 reflectance and the differential detector MO scanning microscopes respectively, for varying degrees of defocus. The responses were generated using the transfer function approach with clear, circular aperture, of equal diameter under uniform incident illumination. The plots have been normalised with respect to the magnitude of the ideal step response (no defocus).
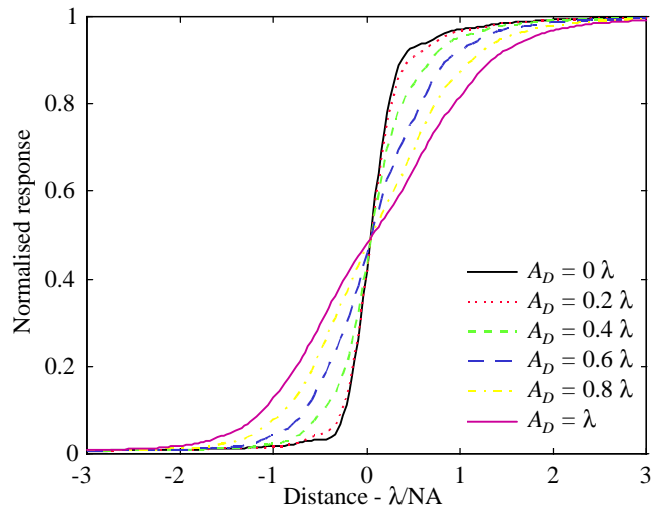

Figure 8.6 : *The step response of the Type 1 reflectance scanning microscope, for varying degrees of defocus.*
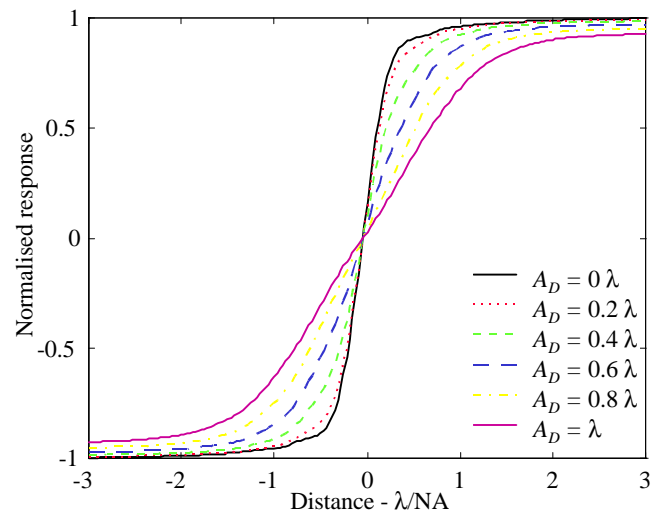
Figure 8.7 : *The step response of the Type 1 differential detector MO scanning microscope, for varying degrees of defocus, for a MO sample of uniform ordinary reflectance and zero phase.*

It is clear that the signal degradation due to defocus is severe. As the amount of defocus is increased the rise-distance of the step responses increases dramatically. In the MO system a reduction in the magnitude of the response is also observed.

8.2.2 Spherical aberration

Spherical aberration is a general term that refers to any type of phase error in an optical system that is symmetrical about the optic axis. The result is that rays travelling through the aperture of the lens at different radii are focused at different points along the optic axis [18].
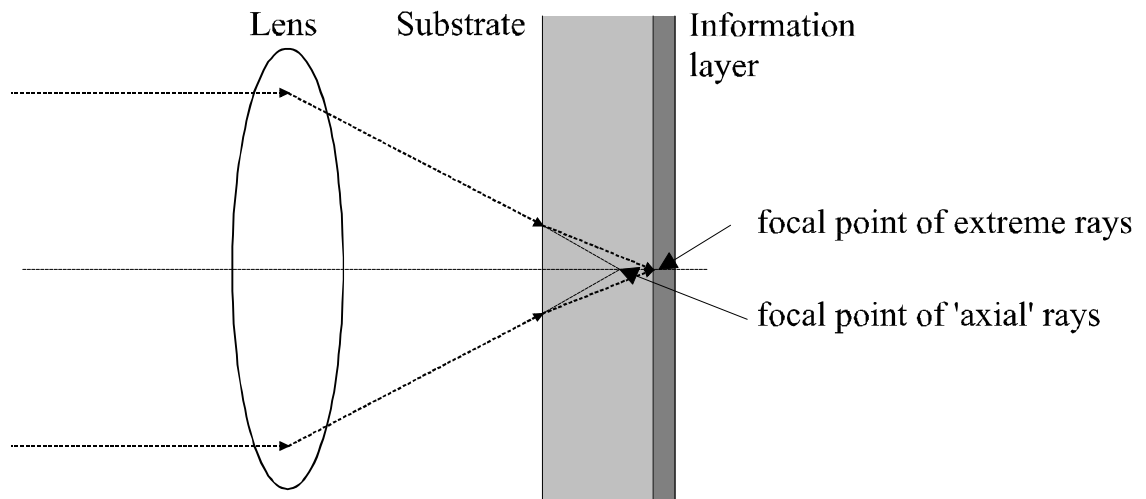

Figure 8.8 : *The origins of spherical aberrations due to focusing through the substrate.*

Spherical aberrations arise in optical storage systems due to the propagation of a non collimated optical wavefront, i.e. the focused field, through the substrate of the optical disc. This results in a bending of the light rays, as illustrated in Fig. 8.8, such that the focal point is shifted.

In the following section the effects of spherical aberrations on the focused spot profile and the response of the scanning microscope is described in detail.

The point spread function with spherical aberration

Figure 8.9 illustrates contour plots of the irradiance profile of a lens for varying degrees of spherical aberration, for a clear circular aperture under uniform illumination. The scale of the plots is in normalised units of λ / NA.
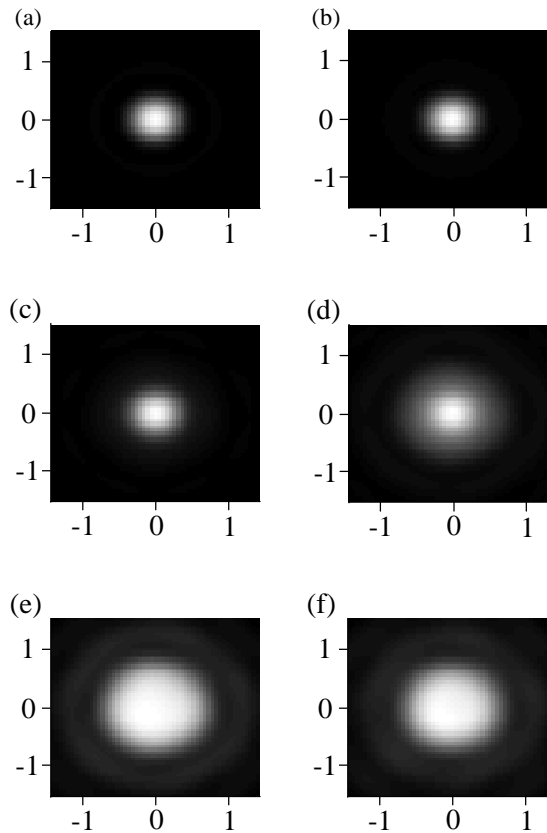

Figure 8.9 : *The irradiance pattern for varying degrees of spherical aberration. Coefficients of spherical aberration, A_s, are a) 0, b) 0.2λ, c) 0.4λ, d) 0.6λ, e) 0.8λ, f) λ.*

In Fig. 8.10 the axial profiles of the irradiance are illustrated normalised with respect to the irradiance of the ideal point spread function (no spherical aberration).

It is apparent that as the amount of spherical aberration is increased the width of the point spread function increases. However, unlike the defocused optical system, the effect of the spherical aberration is to broaden the focused spot profile, without increasing the contribution due to the outer rings. Figure 8.10 clearly illustrates that as

the spherical aberration is increased the peak irradiance reduces. This result is similar to that observed in the case of defocus.
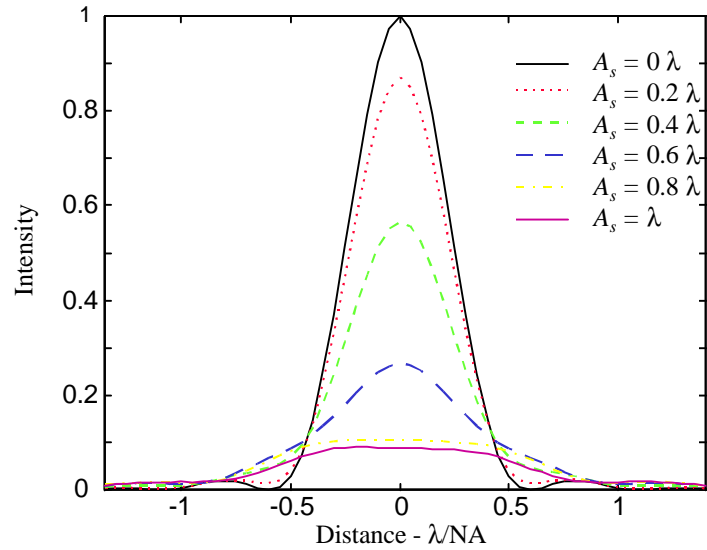

Figure 8.10 **:** *The irradiance profile for varying degrees of spherical aberration.*

The Type 1 PCTF with spherical aberration

Figure 8.11 illustrates the axial form of the Type 1 PCTF, for varying degrees of spherical aberration. The PCTFs were generated using the Type 1 PCTF algorithm with clear, circular apertures, of equal diameter under uniform incident illumination. Again, the spherical aberration is included in both the objective and collector aperture pupil functions.
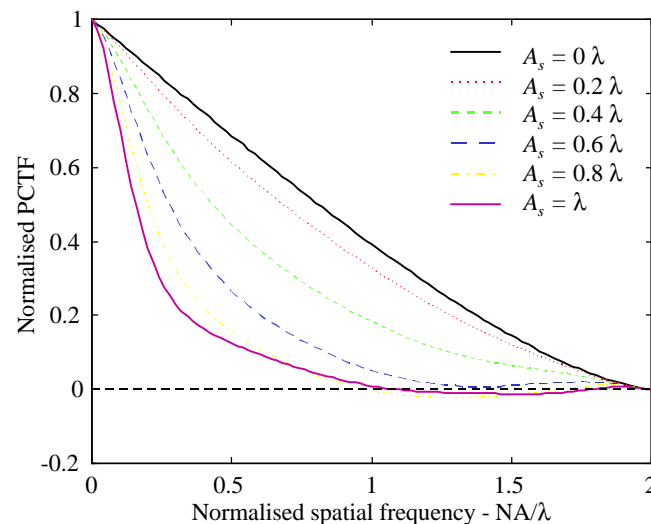

Figure 8.11 : *Normalised PCTFs for varying degrees of spherical aberration.*

It can be seen that unlike the defocused optical system, spherical aberrations produce little contrast reversal in the image. Increasing the amount of spherical aberration merely attenuates the high spatial frequency response of the imaging system, thus reducing the effective cut-off spatial frequency of the imaging system.

The step response of the optical system with spherical aberration

Figures 8.12 and Fig. 8.13 illustrate the step response of the Type 1 reflectance and the differential detector MO scanning microscopes, for varying degrees of spherical aberration, generated using the transfer function approach with the conditions outlined in table 8.1. The plots have been normalised with respect to the magnitude of the ideal step response (no spherical aberration). As the amount of spherical aberration is increased then the response is degraded leading to a increase in the rise-distance of the step response. A similar result to that observed for the effects of defocus.
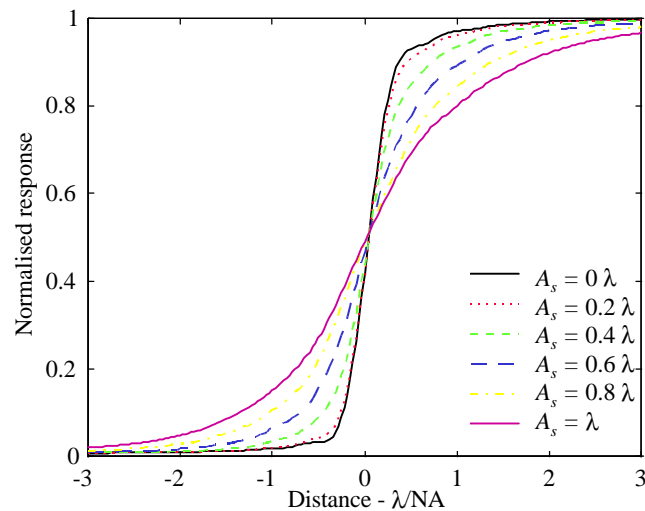

Figure 8.12 : *The step response of the Type 1 reflectance scanning microscope, for varying degrees of spherical aberration.*

The effects of spherical aberrations are often eliminated by taking into account the effect of focusing through a thick transparent substrate when designing the lens [18,60]. Alternatively, the effects of spherical aberrations are sometimes corrected by deliberately defocusing the optical system, such that the contributions due to the spherical aberration and defocus are balanced out [18,107].
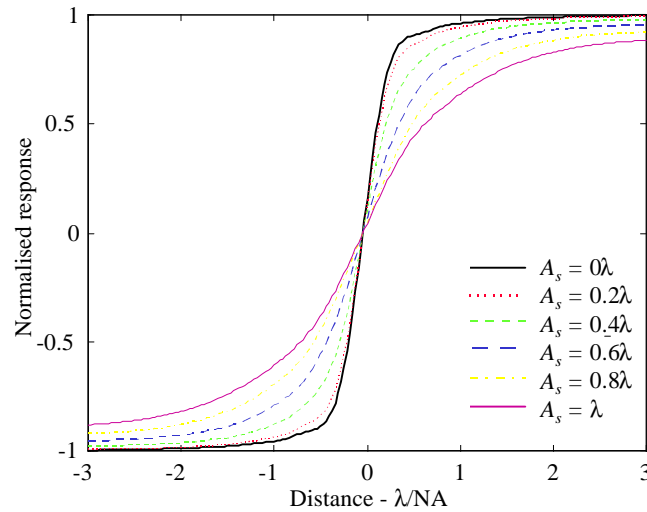
Figure 8.13 : *The step response of the Type 1 differential detector MO scanning microscope, for varying degrees of spherical aberration, for a MO sample of uniform ordinary reflectance and zero phase.*

8.2.3 Astigmatism : substrate birefringence

Astigmatism in optical storage systems is introduced by the anisotropic birefringent properties of the polycarbonate substrate of the optical disc [18,60]. The birefringence affects the polarisation state of the propagating wavefront, such that the overall system performance is degraded by the introduction of readout signal fluctuations [18,75,111,112,117]. Substrate birefringence causes signal degradation particularly in magneto-optic systems, where the signal is dependent upon the phase characteristics of the reflected polarised field.

Birefringence arises in the optical disc substrate due to the substrate material having different refractive indices in the radial (across the track), n_r, tangential (along the track), n_t, and vertical (normal to the plane of the disc), n_n, directions, as illustrated in Fig. 8.14.

Substrate birefringence is often expressed in terms of the lateral birefringence (in the plane of the disc) and vertical birefringence (vertical to the disc). In MO systems the polarisation vector of the incident beam is typically aligned along the track. Upon reflection from the MO film there exists an orthogonal polarisation component

introduced by the magneto-optic Kerr effect. The phase shift between the two orthogonal components is affected by both the lateral and vertical birefringent properties of the disc substrate. The effects introduced by the lateral birefringence can cause significant signal degradation in the magneto-optic readout channel by changing the polarisation state of the reflected beam so it becomes elliptical, thus lowering the signal to noise ratio of the readout signal [108,109,112,114,120]. However, the effects of lateral birefringence can be effectively removed by the introduction of a wave-plate into the readout channel of the optical system, the axis of which can be aligned to remove the phase shift introduced by the lateral birefringence.
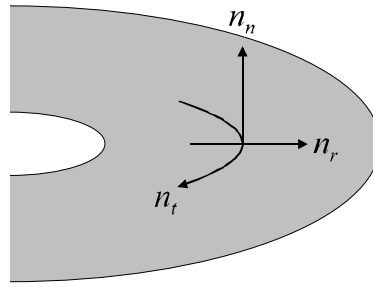

Figure 8.14 : *Birefringent properties of the optical disc substrate.*

Vertical birefringence, however, cannot be easily removed since it introduces astigmatism into the reflected beam [109,113]. As a first approximation the effects of vertical birefringence can be modelled by introducing an aberration function due to astigmatism into the aperture pupil function of the objective lens, i.e.

$$W(\boldsymbol{r},\boldsymbol{f}) = \left(-\frac{\Delta n_z D N A^2}{n^2}\right)\boldsymbol{r}^2 \cos^2\left(\boldsymbol{f}-\boldsymbol{p}/2\right) \tag{8.11}$$

for an incident field linearly polarised in across the track, and

$$W(\boldsymbol{r},\boldsymbol{f}) = \left(-\frac{\Delta n_z D N A^2}{n^2}\right)\boldsymbol{r}^2 \cos^2\left(\boldsymbol{f}\right) \tag{8.12}$$

for an incident field linearly polarised in along the track, where Δn_z is the vertical birefringence, D is the thickness of the substrate, NA is the numerical aperture of the objective lens, and n is the average birefringence of the substrate [75,115]. It should be noted that to investigate fully the effects due to substrate birefringence vector

diffraction analysis must be performed, which is beyond the scope of this work [75,108,109,116].

In the following section the effects of astigmatism on the focused spot profile and the response of the scanning microscope is investigated.

The point spread function with astigmatism

Figure 8.15 shows the irradiance pattern from of a lens for varying degrees of astigmatism, for a clear circular aperture under uniform illumination, the scale of the plots being in normalised units of l / NA. Figure 8.16 depicts the axial profiles of the irradiance, normalised with respect to the irradiance of the ideal case (no astigmatism).
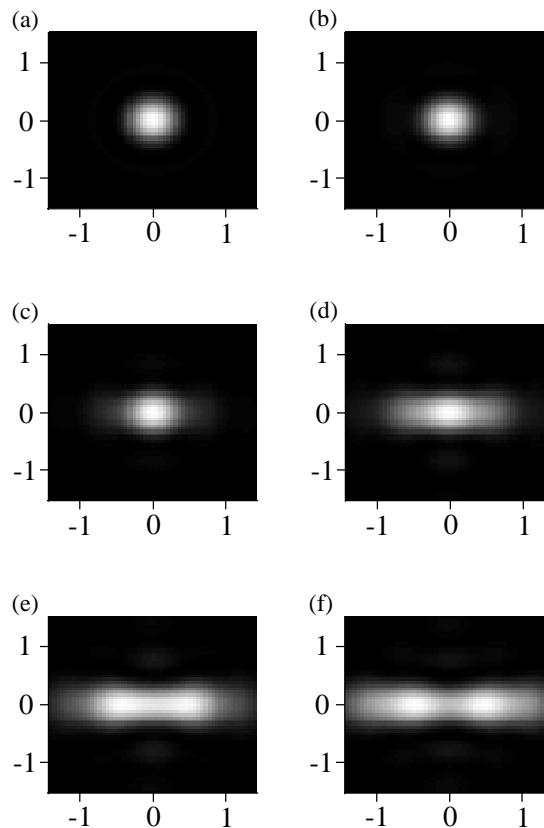

Figure 8.15 : *The irradiance profile for varying degrees of astigmatism. Coefficients of astigmatism, A_A, are a) 0, b) 0.2l, c) 0.4l, d) 0.6l, e) 0.8l, f) l.*
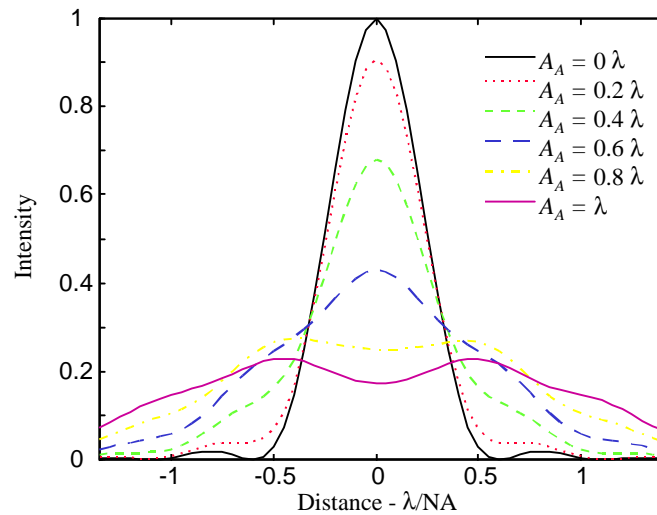
Figure 8.16 : *The profile of the Airy disc point spread function for varying degrees of astigmatism.*

Figures 8.15 and 8.16 illustrate that the effects of astigmatism on the focused spot differ greatly compared with the other forms of aberrations discussed. Astigmatism causes a broadening of the focused spot along a particular direction, unlike defocus and spherical aberrations which caused a circularly symmetrical broadening of the focused spot. An interesting result is illustrated in Fig. 8.15 (f) where the focused spot profile is formed by effectively two smaller spots displaced by approximately λ/NA.

The Type 1 PCTF with astigmatism

Figure 8.17 illustrates the axial form of the Type 1 PCTF, for varying degrees of astigmatism, generated using the Type 1 PCTF algorithm with clear, circular apertures of equal diameter under uniform incident illumination. Astigmatism is included in both the objective and collector aperture pupil functions. The magnitude of high spatial frequency components rapidly attenuates, and becomes negative, as the amount of astigmatism is increased, leading to a loss in resolution and large amounts of contrast reversal in the output image.
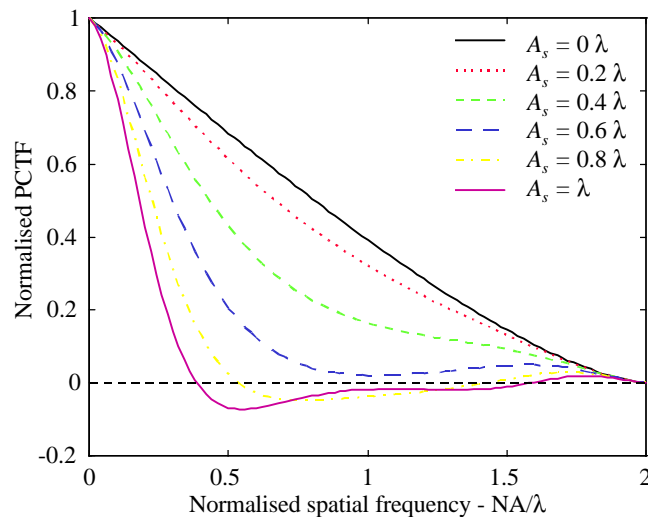
Figure 8.17 : *Normalised PCTFs for varying degrees of astigmatism.*

The step response of the optical system with astigmatism

Figure 8.18 and Fig. 8.19 illustrate the normalised step response of the Type 1 reflectance and the differential detector MO scanning microscopes, for varying degrees of astigmatism, generated using the transfer function approach with the conditions outlined in table 8.1.
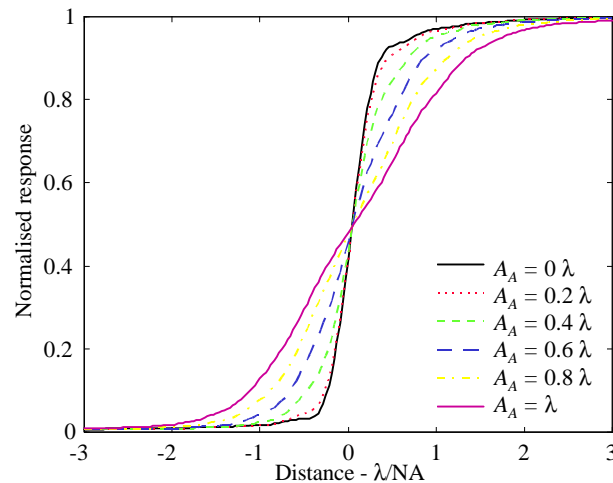

Figure 8.18 : *The step response of the Type 1 reflectance scanning microscope, for varying degrees of astigmatism.*

The effects due to astigmatism on the readout signal from optical systems, is similar to that generated for defocus and spherical aberration. However, it must be noted that

the response depends on the orientation of the electric field vector with respect to the orientation of the polymeric chains of the disc substrate [114].
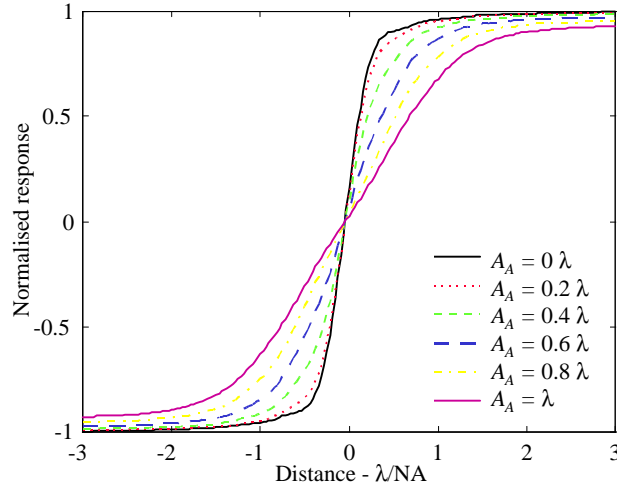

Figure 8.19 : *The step response of the Type 1 differential detector MO scanning microscope, for varying degrees of astigmatism for a MO sample of uniform ordinary reflectance and zero phase.*

8.2.4 Additional aberrations

It has been illustrated how the common forms of primary aberrations, defocus, spherical aberration and astigmatism, can be modelled with respect to imaging in optical storage systems. The other forms of primary aberrations : coma and tilt, can also be modelled using the same approach.

Coma is caused by the passage of a non-collimated beam through a tilted plate, lens or beamsplitter. Coma effects the focused spot by introducing a diffuse tail, such that it resembles a comet, hence, coma. Since, the optical beam in optical storage systems is almost always collimated, then the effects due to coma are insubstantial [5]. The effects of tilt are often included in the analysis of coma.

More than one aberration may be evident in an optical system at any one time. This may further degenerate the response of the system, or may in fact improve the response if the effects of the aberrations cancel out, such as for certain combinations

of defocus and spherical aberrations. The effects of combinations of primary aberrations has been presented elsewhere [107].

It should be noted that a high NA optical system is more sensitive to aberrations, and that as the wavelength of illumination is reduced the effects of aberrations increase even more. Hence, it is important in the design of future storage technologies that the effects of aberrations are clearly understood [18,108].